Theory of quarter-wave-stack dielectric mirrors used in a thin Fabry–Perot filter

Elsa Garmire

I present a new derivation of the analytic form for the phase shift near resonance and the optical penetration length upon reflection from a distributed dielectric mirror consisting of a quarter-wave stack. The requirement of proper termination to achieve high reflectivity is suspended to investigate large optical penetration depths. Separate equations, derived for N and $N + 1/2$ layer pairs, are convenient for the design of tunable Fabry–Perot filters with a specified tuning range. The analysis is also applicable to distributed Bragg reflectors, vertical-cavity surface-emitting lasers, and resonant photodiodes. I show that the penetration length can sharply reduce the overly broad free spectral range of an ultrathin Fabry–Perot filter that might be useful in applications such as tunable wavelength filters for wavelength division multiplexing applications. The results also demonstrate regimes of zero dispersion and of superluminal reflection in the dielectric mirrors, which are of particular interest in photonic bandgap structures.

OCIS codes: 120.2230, 120.5700, 140.4780, 120.2440, 230.4040.

1. Introduction

A Fabry–Perot filter has been proved to be a useful tunable wavelength filter for fiber-optic applications.[1–4] Because of the distributed reflection of the quarter-wave-stack (QWS) dielectric mirror, it is necessary to include the reflection phase in calculation of the modes of these Fabry–Perot (FP) filters. Dispersion in this phase leads to an optical penetration length L_M within the mirror that must be included in the FP analysis. This penetration length can be made large if the geometry is properly chosen; this choice, however, also lowers the reflectivity of the mirror and has not typically been considered in applications that require ultrahigh reflectivity, such as vertical-cavity surface-emitting lasers. One application that appears promising for large L_M is in the design of tunable FP's filters with a specified tuning range for which this analytic form for L_M is convenient. The analysis is also applicable to vertical-cavity surface-emitting lasers and can be considered an extension of the analytic solution of Babic and Corzine.[5] These authors derived the equation for L_M under the assumption of mirror geometries that give large reflectivity, a geometry they call *properly terminated*. The analysis presented here extends their results to include mirrors that are *arbitrarily terminated*. That is, the equations have been derived for either high reflectivity and low phase dispersion or low reflectivity and high phase dispersion. Numerical calculations confirm the validity of the results presented here for QWSs with arbitrary termination.

Here I use the terminology QWS, but distributed Bragg reflector (DBR) could also be used, and this analysis applies to DBR mirrors as well. There is an exact correspondence between the matrix multiplication approach for solving the QWS and the coupled mode approach for solving the DBR,[6,7] as was also pointed out in Ref. 5. More recently Brovelli and Keller[8] used this approach to obtain the optical penetration length in terms of coupling coefficients.

Because of the generality of the derivation given here, we can clarify the effect of the order in which the films are deposited on the tuning range of a FP filter, that is, the effect of termination on reflectivity and phase dispersion. Similarly, N and $N + 1/2$ layers are compared. We derive conditions for large values of L_M. Most importantly, we also find regimes of optical length $L_M \leq 0$ in the QWS, which implies superluminal reflection and is applicable to photonic bandgap materials.[9]

The author is with the Thayer School of Engineering, 3000 Cummings Hall, Dartmouth College, Hanover, New Hampshire 03755. Her e-mail address is garmire@dartmouth.edu.

Received 21 November 2002; revised manuscript received 30 May 2003.

0003-6935/03/275442-08$15.00/0

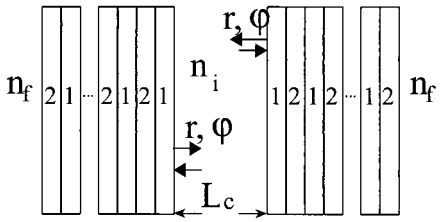

Fig. 1. Geometry for symmetric FP cavity of physical length L_c with an internal refractive index of n_i and identical QWS mirrors each consisting of N quarter-wave layer pairs of alternating refractive indices n_1 and n_2. The final refractive index outside the QWS is n_f. The internal electric field observes a reflection coefficient of $r \exp(i\varphi)$ at each QWS mirror. All the refractive indices can have any values, and the extension to an asymmetric cavity is straightforward.

2. Fabry–Perot Analysis

A. Mode Spacing with Quarter-Wave-Stack Dielectric Mirrors

Consider the symmetric FP filter shown in Fig. 1, composed of two QWS dielectric mirrors with reflection coefficients $r \exp(i\varphi)$ separated by a physical cavity length L_c, where phase φ is defined as measured from the front surface of each mirror. Extension to asymmetric cavities is trivial. Let the optical path length (OPL) of the FP filter be $L_{\mathrm{OPL}} = n_i L_c$. The FP modes require the round-trip phase to be an integral number of 2π:

$$2k_m L_{\mathrm{OPL}} + 2\varphi_m = m2\pi, \tag{1}$$

where $k_m = 2\pi/\lambda_m$, the mth mode of this FP filter. In general there is a wavelength dependence of refractive indices that is due to material dispersion, but it will be ignored, as justified later. When the cavity is filled with air this is a good approximation. In many cases this cavity could be filled with an active or nonlinear medium and n_f might be air.

Consider a new cavity mode $m + 1$ with a new wavelength $\lambda_{m+1} = \lambda_m - \Delta\lambda_{\mathrm{FSR}}$, where FSR stands for free spectral range. The wave vector becomes $k_{m+1} = k_m + \Delta k_{\mathrm{FSR}}$ and the phase of the dielectric mirror reflection coefficient becomes $\varphi_{m+1} = \varphi_m + \Delta\varphi_{\mathrm{FSR}}$. We show below that $\partial\varphi/\partial k$ is constant over much of the wavelength region of a dielectric mirror. Writing $\Delta\varphi_{\mathrm{FSR}} = (\partial\varphi/\partial k)\Delta k_{\mathrm{FSR}}$, one can subtract Eq. (1) and its equivalent expression for mode $m + 1$ to obtain $2\Delta k_{\mathrm{FSR}} L_{\mathrm{OPL}} + 2(\partial\varphi/\partial k)\Delta k_{\mathrm{FSR}} = 2\pi$. This leads to

$$\Delta k_{\mathrm{FSR}} = \frac{\pi}{L_{\mathrm{OPL}} + \partial\varphi/\partial k}. \tag{2}$$

The form of Eq. (2) shows that dispersion in the phase of the reflection coefficient of the QWS effectively changes the OPL of the FP filter, so that the mode spacing is given simply by

$$\Delta k_{\mathrm{FSR}} = \pi/L_{\mathrm{eff}}. \tag{3}$$

To allow for a cavity that is not symmetric but has mirrors a and b, replace $\partial\varphi/\partial k$ by its average over both mirrors, and

$$\begin{aligned} L_{\mathrm{eff}} &= L_{\mathrm{OPL}} + L_{Ma} + L_{Mb} \\ &= L_{\mathrm{OPL}} + (1/2)\partial\varphi_a/\partial k + (1/2)\partial\varphi_b/\partial k. \end{aligned} \tag{4}$$

Thus standard FP analyses can be applied to find the mode spacing, as long as the FP length is taken as the optical path length L_{eff}. This result is expected because of the finite penetration length into the distributed mirror[5]; in this paper I derive an analytic expression for $\partial\varphi/\partial k = 2L_M$ that allows Eq. (4) to be calculated in a simple way.

B. Wavelength Tuning Range

A FP filter with a transmission resonance at λ_m has a tunability window for the cavity that is no more than half of a FSR to either side of λ_m before the next mode comes in and interferes with the signal. The minimum and maximum wavelengths in the tuning range correspond to $k_m + \Delta k_{\mathrm{FSR}}/2$ and $k_m - \Delta k_{\mathrm{FSR}}/2$, respectively, where $\Delta k_{\mathrm{FSR}} = \pi/L_{\mathrm{eff}}$. The maximum and minimum wavelengths in the tuning range to either side of the central wavelength λ_m are

$$\lambda_- = 2\pi(k_m - \pi/2L_{\mathrm{eff}})^{-1} = (1/\lambda_m + 1/4L_{\mathrm{eff}})^{-1}, \tag{5}$$

$$\lambda_+ = 2\pi(k_m + \pi/2L_{\mathrm{eff}})^{-1} = (1/\lambda_m - 1/4L_{\mathrm{eff}})^{-1}. \tag{6}$$

The total tuning range is the difference between these two:

$$\lambda_+ - \lambda_- = \lambda_m(\lambda_m/2L_{\mathrm{eff}})[1 - (\lambda_m/4L_{\mathrm{eff}})^2]^{-1}. \tag{7}$$

The correction term in the last factor is not important except for very thin FP filters; the tuning range is approximately half of the FSR.

3. Quarter-Wave-Stack Dielectric Mirror Analysis

A. Matrix Method

A particularly convenient way to analyze optical transmission through a stack of dielectric films is to use real matrices for each layer.[10] As shown in Fig. 1, light enters each layer pair first into medium 1 with refractive index n_1 and then into medium 2 of refractive index n_2. As shown in Ref. 10, such a layer pair has the following transmission matrix:

$$\begin{aligned} M_P &= M_1 M_2 \\ &= \begin{bmatrix} \cos\vartheta_1 & \sin\vartheta_1/n_1 \\ -n_1\sin\vartheta_1 & \cos\vartheta_1 \end{bmatrix} \begin{bmatrix} \cos\vartheta_2 & \sin\vartheta_2/n_2 \\ -n_2\sin\vartheta_2 & \cos\vartheta_2 \end{bmatrix}, \end{aligned} \tag{8}$$

where $\vartheta_j = kn_jL_j$ and n_jL_j is the optical path length in each film layer ($k = 2\pi/\lambda$ is an arbitrary free-space wave vector). For a dielectric mirror on resonance, all ϑ_j terms are equal to $\pi/2$, and we define the mirror resonance wave vector k_o. If there are N identical

pairs of layers, the matrices in Eq. (8) can be generalized to

$$M_N = (M_1 M_2)^N. \tag{9}$$

Once this matrix is calculated, it can be expressed as

$$M_N = \begin{bmatrix} M_{00} & M_{01} \\ M_{10} & M_{11} \end{bmatrix}, \tag{10}$$

from which the reflection and the transmission coefficients are determined. These equations differ from those usually found in textbooks because real matrices are used rather than complex matrices, which simplifies the analysis of complex structures. In this formulation the reflection coefficient is[10] (the reference has a sign misprint that is corrected here)

$$r = \frac{(iM_{00} + n_f M_{01})n_i - (in_f M_{11} - M_{10})}{(iM_{00} + n_f M_{01})n_i + (in_f M_{11} - M_{10})}, \tag{11}$$

where n_i is the initial refractive index, that is, the medium from which the light enters into layer 1 with refractive index n_1. And n_f is the final refractive index, that is, the medium into which the light exits after it passes through the last layer. For N layer pairs, the last layer will have a refractive index n_2, whereas for $N + 1/2$ layer pairs the last layer will have a refractive index n_1.

The transmission coefficient is

$$t = \frac{-2in_i n_f}{(iM_{00} + n_f M_{01})n_i + (in_f M_{11} - M_{10})}. \tag{12}$$

These equations have been checked against the approach of Born and Wolf[11] and they agree exactly. From Eq. (11) the reflectivity becomes

$$R = |r|^2 = \frac{(n_i n_f M_{01} + M_{10})^2 + (M_{00} n_i - n_f M_{11})^2}{(n_i n_f M_{01} - M_{10})^2 + (M_{00} n_i + n_f M_{11})^2}, \tag{13}$$

and, of course, $R + |t|^2/n_f = 1$. Algebra shows that the phase of Eq. (11) is given by

$$\tan \varphi = \frac{-2n_i(M_{00}M_{10} + n_f^2 M_{11}M_{01})}{(n_i n_f M_{01})^2 - M_{10}^2 + (M_{00}n_i)^2 - (n_f M_{11})^2}. \tag{14}$$

In general this phase expression can be evaluated numerically. However, because the FP filter usually operates at wavelengths near the resonance wavelength of the QWS, a simple analytic result can be obtained.

Figure 2 shows a plot of phase φ and mirror reflectivity R as functions of fractional wave-vector deviation from resonance $\delta k/k$. Phase φ is essentially linear as long as $\varphi < \pi/4$, which for this case corresponds to $\delta k/k < 0.1$. The reflectivity remains high in this same regime as long as $\varphi < \pi/4$. We can calculate the slope of this phase φ near resonance by carrying out an appropriate Taylor expansion and from this determine the optical mirror penetration length L_M. For wavelengths sufficiently near resonance that reflectivity is high, this is a good estimation of L_M.

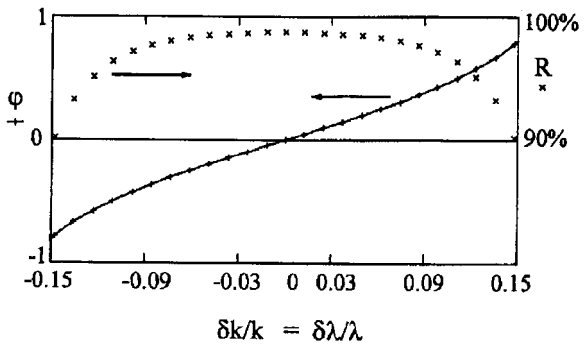

Fig. 2. Phase of the total reflection coefficient φ (solid curve) and reflectivity R (crosses) as a function of fractional wave-vector deviation $\delta k/k_o$ (or fractional wavelength deviation $\delta\lambda/\lambda_o$). The peak value of the reflectivity shown here is $R_o = 0.988$. The graph is drawn assuming the number of layer pairs $N = 5$, and the refractive indices are $n_1 = 2.2$, $n_2 = 1.4$, $n_i = 1$ and $n_f = 3.45$.

B. Near Resonance

Near resonance $n_j L_j \approx \lambda_o/4$, where λ_o is the resonant wavelength, so that $\vartheta_j \approx (2\pi/\lambda_o)(\lambda_o/4) \approx \pi/2$. When the wavelength is slightly off resonance, we can write $\vartheta_j = \pi/2 + \delta_j$. Thus $\cos \vartheta_j = -\sin \delta_j \approx -\delta_j$ and $\sin \vartheta_j = \cos \delta_j = 1 - \delta^2/2$. The matrix for each individual layer becomes

$$M = \begin{bmatrix} -\delta_j & (1 - \delta_j^2/2)/n \\ -n(1 - \delta_j^2/2) & -\delta_j \end{bmatrix}. \tag{15}$$

Calculating a layer pair, expanding in a power series in δ_j, but keeping only those terms linear in δ yield

$$M_P = \begin{bmatrix} -n_2/n_1 & -\delta_1/n_2 - \delta_2/n_1 \\ \delta_2 n_1 + \delta_1 n_2 & -n_1/n_2 \end{bmatrix}. \tag{16}$$

Chromatic aberration can be ignored because the phase varies as the slope of the logarithm of the refractive index, as shown next. When the wave vector becomes $k_o + \delta k$, the phase accumulated as it travels through each layer changes by $\delta_1 = \{n_1 L_1 + k_o n_1 L_1[(\partial n_1/\partial k)/n_1]\}\delta k$. In an ideal QWS, each layer has $n_1 L_1 = n_2 L_2 = \lambda_o/4 = \pi/2k_o$. We can also write

$$\begin{aligned} k_o[(1/n_1)(\partial n_1/\partial k)] &= k_o\{[\partial \ln(n_1)/\partial k]\} \\ &= \lambda_o[\partial \ln(n_1)/\partial \lambda], \end{aligned}$$

so

$$\delta_1 = \{1 + \lambda[\partial \ln(n_1)/\partial \lambda]\}(\pi/2)(\delta k/k_o). \tag{17}$$

Because this is a logarithmic dependence on chromatic dispersion, it is small and can usually be ignored. If it cannot be ignored, then $\delta_1 \neq \delta_2$, and this shows up as slight corrections to n_1 and n_2 in Eq. (16). Material dispersion is ignored in what follows, and it is assumed that $\delta_1 = \delta_2 = \delta \equiv \vartheta_j - \pi/2 = (\pi/2)(\delta k/k_o)$.

C. Phase Change for N Layer Pairs Near Resonance

The matrix element for each layer pair to lowest order in δ can be written as

$$M_P = (-1)\begin{bmatrix} a & b\delta \\ -c\delta & d \end{bmatrix}, \tag{18}$$

where $a = n_2/n_1$, $b = (1/n_1 + 1/n_2)$, $c = (n_1 + n_2)$, and $d = n_1/n_2$. To first order the diagonal elements have no wavelength dependence whereas the off-diagonal elements are proportional to δ.

The matrix for two layer pairs to order δ is

$$M_2 = \begin{bmatrix} (n_2/n_1)^2 & (1/n_1 + 1/n_2)(n_2/n_1 + n_1/n_2)\delta \\ -(n_1 + n_2)(n_2/n_1 + n_1/n_2)\delta & (n_1/n_2)^2 \end{bmatrix}. \tag{19}$$

Note that to order δ the diagonal elements again have their resonance values. The off-diagonal elements are again proportional to δ. Because of the first-order Taylor approximation, this will be true no matter how many layer pairs there are. As a result, Eq. (14) shows that the tangent of the phase is linear around resonance, as assumed in Eq. (4).

The phase change for reflection from a QWS that consists of N layer pairs can now be written to first order in δ. Using the notation from above, the on-resonance diagonal terms are well known to be a^N and d^N; define the off-diagonal terms with N layer pairs as $b_N\delta$ and $-c_N\delta$. Then, also ignoring the δ^2 orders in the denominator,

$$\tan \varphi_N = 2n_i \frac{a^N c_N - n_f^2 d^N b_N}{n_i^2 a^{2N} - n_f^2 d^{2N}}\,\delta. \tag{20}$$

On resonance $\delta = 0$ and $\tan \varphi_N = 0$, so the on-resonance phase of a QWS that consists of N layer pairs is $\varphi_N = 0$ or π. For small deviations, $\tan \varphi_N \approx \delta\varphi$. We used $\delta \equiv (\pi/2)(\delta k/k_o)$ to obtain

$$\delta\varphi = 2n_i \frac{a^N c_N - n_f^2 d^N b_N}{n_i^2 a^{2N} - n_f^2 d^{2N}}\,(\delta k/k_o)(\pi/2). \tag{21}$$

This verifies the idea that φ is linearly proportional to wave vector k, as shown in Fig. 2. Such linearity has been verified experimentally.[12]

Continued multiplication shows that for N layer pairs the off-diagonal coefficients b_N and c_N are given by

$$b_N = b(a^{N-1} + a^{N-2}d + a^{N-3}d^2 \ldots ad^{N-2} + d^{N-1}) \equiv bF_N, \tag{22}$$

$$c_N = c(a^{N-1} + a^{N-2}d + a^{N-3}d^2 \ldots ad^{N-2} + d^{N-1}) \equiv cF_N, \tag{23}$$

where

$$F_N = a^{N-1} + a^{N-3} + a^{N-5} \ldots a^{-N+3} + a^{-N+1}, \tag{24}$$

where $a = n_2/n_1$. F_N can be simplified by writing

$$a^{N-1}F_N = (a^2)^{N-1} + (a^2)^{N-2} + \ldots 1 = (a^{2N} - 1)/(a^2 - 1). \tag{25}$$

Inserting these results into the equation for the phase as a function of $\delta \equiv \delta\vartheta$ yields

$$\delta\varphi/\delta\vartheta = 2\,\frac{n_1 n_2[1 - (n_f^2/n_1 n_2)a^{-2N}](1 - a^{-2N})}{n_i(n_2 - n_1)[1 - (n_f/n_i)^2 a^{-4N}]}, \tag{26}$$

where $a \equiv n_2/n_1$. Equation (26) has been tested with numerical calculations and the linear approximation does not break down until $\varphi \approx \pi/4$. Equation (26) is exactly valid on resonance for any combination of refractive indices, since it was derived by a Taylor expansion.

D. Result for Effective Mirror Length L_M

The result of Eq. (26) should be plugged into Eq. (4) to find the optical cavity length in the presence of QWS mirrors. From Eq. (4) we can define an increase in the OPL for the FP filter that is due to each mirror: $L_M \equiv (1/2)(\partial\varphi/\partial k)$. Write $\partial\varphi/\partial k = (\delta\varphi/\delta\vartheta)(\delta\vartheta/\delta k)$ and use $\delta\vartheta/\delta k = n_j L_j = \lambda_o/4$ to obtain

$$L_M \equiv (\delta\varphi/\delta\vartheta)(\lambda_o/8), \tag{27}$$

where $(\delta\varphi/\delta\vartheta)$ is given by Eq. (26).

Thus the effective single-pass increase in OPL that is due to dispersion in the phase of the reflectivity of a QWS mirror with N layer pairs is

$$L_M = \frac{n_1 n_2[1 - (n_f^2/n_1 n_2)(n_1/n_2)^{2N}][1 - (n_1/n_2)^{2N}]}{n_i(n_2 - n_1)[1 - (n_f/n_i)^2(n_1/n_2)^{4N}]}\,(\lambda_o/4). \tag{28}$$

This can be compared with the result given by Babic and Corzine[5] if we combine their Eqs. (21) and (26) under their conditions $n_i < n_1$, $n_1 < n_2$, and $n_f < n_2$. Their equations give a one-way OPL of

$$n_i L_T = (c/2)(1/2\nu)(n_1/n_i)\,\frac{n_2}{(n_2 - n_1)} \times \frac{[1 - (n_f/n_2)^2(n_1/n_2)^{m-1}][1 - (n_1/n_2)^m]}{[1 - (n_1/n_i)^2(n_f/n_2)^2(n_1/n_2)^{2m-2}]}, \tag{29}$$

where ν is the frequency. Use of $m = 2N$ can simplify Eq. (29) to the exact same form as in Eq. (28), since $c/\nu = \lambda_o$. Thus here we have derived the OPL by using a method that makes no assumptions as to which refractive indices are large and which are small.

The approach offered here is complementary to that of Babic and Corzine.[5] Their derivation uses the time domain and our derivation uses the frequency domain. Their result is interpreted as a time delay in an optical pulse when reflected from a QWS. Our result is a phase difference between on-resonance and off-resonance frequencies of the Bragg reflector. A Fourier transform analysis, similar to that which derives group velocity from refractive-index dispersion, will show that both approaches are analogous.

When $(n_1/n_2)^{2N} \ll 1$, a Taylor expansion of Eq. (28) to first order gives

$$L_{LH} = \frac{n_1 n_2}{n_i(n_2 - n_1)}\{1 - [(n_f^2/n_1 n_2) + 1](n_1/n_2)^{2N}\}(\lambda_o/4), \tag{30a}$$

for $n_2 \gg n_1$ and large N. In contrast, when $(n_1/n_2)^{2N} \gg 1$,

$$L_{HL} = \frac{n_i}{n_1 - n_2}\{1 - [(n_1 n_2/n_f^2) + 1](n_2/n_1)^{2N}\}(\lambda_o/4), \tag{30b}$$

for $n_2 \ll n_1$ and large N. Not surprisingly, L_M is smaller for a finite number of layers than the infinite limit, which was also shown by Ref. 5. Agreement to within 10% in most practical cases is found with these simplified versions. In the limit $N \to \infty$, $L_{LH} = (n_1 n_2/n_i^2)L_{HL}$.

E. On-Resonance Reflectivity

The on-resonance reflectivity for this mirror with N layer pairs will be

$$R_N = \frac{(n_i a^N - n_f d^N)^2}{(n_i a^N + n_f d^N)^2} = \frac{[1 - (n_f/n_i)(n_1/n_2)^{2N}]^2}{[1 + (n_f/n_i)(n_1/n_2)^{2N}]^2}, \tag{31}$$

and the reflectivity is less than unity by the transmission loss:

$$T_N = 1 - R_N = \frac{4}{(n_i/n_f)(n_2/n_1)^{2N} + (n_f/n_i)(n_1/n_2)^{2N} + 2}. \tag{32}$$

Compare reflection loss for the two orderings when $N \gg 1$:

$$T_{\mathrm{HL}} = (4n_i/n_f)(n_2/n_1)^{2N}, \tag{33a}$$

for $n_1 \gg n_2$ and large N;

$$T_{\mathrm{LH}} = 4(n_f/n_i)(n_1/n_2)^{2N}, \tag{33b}$$

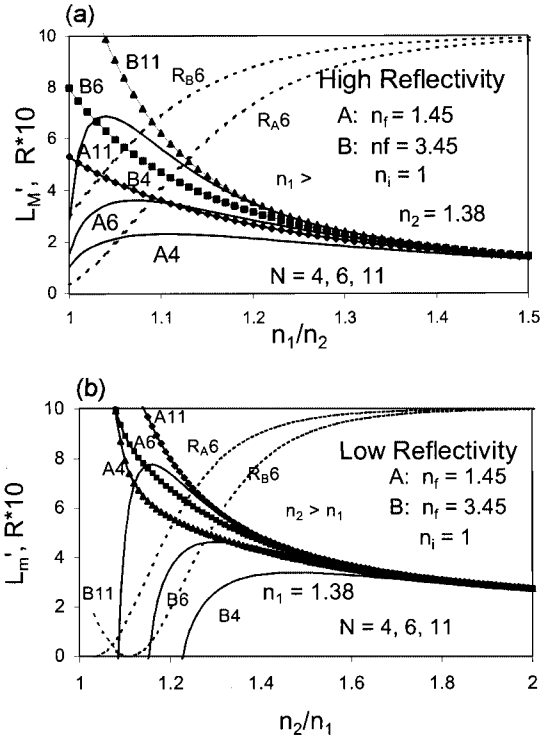

Fig. 3. Normalized optical mirror penetration length L_M (in units of $\lambda_o/4$) for several different numbers of layer pairs N and for two cases in which n_f differs. Also shown are typical reflectivities for both cases R_A and R_B (for $N = 6$ layer pairs). Light is incident from the air: (a) HL configuration with $n_1 = 1.38$ and a varying ratio of n_2/n_1 and (b) LH configuration with $n_2 = 1.38$ and a varying ratio of n_1/n_2.

for $n_2 \gg n_1$ and large N. For $n_i < n_f$ (and a given number of layer pairs), the first case in which the ordering is high–low (HL) gives the smallest transmission loss (highest reflectivity), with n_i/n_f as small as possible. This case also gives the smallest optical penetration length L_M [Eq. (28)]. Thus higher reflectivity implies smaller L_M. If larger L_M is sought, the reflectivity will be smaller.

F. Limit of Validity of Approximation

The approximation leading to the analytic result is valid for $\varphi < \pi/4$. This can be referred back to fractional wave-vector deviation if we set $\delta\varphi < \pi/4$ and by use of $\delta k = \delta\varphi/2L_M = (\pi/4)/2L_M$. Thus the approximation is valid when

$$\frac{\delta k}{k_o} < \frac{\lambda_o}{16 L_M}. \tag{34}$$

By use of the same configuration as in Fig. 1, Eq. (28) shows $L_M = 0.96$ μm (for $\lambda = 1.55$ μm), so Eq. (34) yields $\delta k/k_o < 0.10$, in good agreement with the regime of linearity of the phase shown in Fig. 1. Equation (34) also yields an analytic expression for the regime over which the reflectivity is large.

G. Plot of Optical Mirror Length L_M

Figure 3 shows normalized values L_M' of the optical

penetration length [$L_M \equiv L_M'(\lambda_o/4)$] versus the ratio of refractive indices with $n_i = 1$ for several different numbers of layer pairs N. Two different values of substrate refractive index are shown: case A with $n_f = 1.45$ corresponding to $n_f^2 < n_1 n_2$, and case B with $n_f = 3.45$ corresponding to $n_f^2 > n_1 n_2$. Also shown for handy reference are the values of the resonance reflectivity for both cases with $N = 6$, labeled R_A6 and R_B6.

Figure 3(a) shows the results when the ordering of the layers is chosen as HL ($n_1 > n_2$), which gives the highest reflectivity. These results agree exactly with those of Ref. 5 and were also confirmed by matrix multiplication to be valid to four decimal places. When the ratio of refractive indices is greater than ~1.5, it can be seen that the curves coalesce, independent of N and of the substrate refractive index. The limit [from Eq. (30b)] is $L_M'(\mathrm{HL}) \rightarrow n_i(n_1 - n_2)^{-1}$. The largest $n_1 - n_2$ might be ~2.5 (GaAs and air), so the smallest that L_{HL} can be is $L_{\mathrm{HLlim}} = 0.4(\lambda_o/4)$, which equals 0.15 μm when light has a wavelength of 1.55 μm.

Figure 3(a) shows that when n_1/n_2 becomes small the normalized penetration length can increase dramatically from its value of ~2 (when $n_1/n_2 = 1.5$) to a value greater than 10 for case B ($n_f = 3.45, N = 11$). However, then the reflectivity dramatically falls off from its high of ~100%. This makes sense because the light extends further and further into the QWS as the refractive-index difference decreases. Indeed, for case B, the limiting large value for L_M' is slightly more than the number of layer pairs. However, for case A the behavior of L_M' with n_1/n_2 is different, going through a peak and approaching zero as $n_1/n_2 \rightarrow 1$. These limiting behaviors can all be found analytically from Eq. (28).

More dramatic behavior is seen in Fig. 3(b) where the layer pair ordering is LH ($n_1 < n_2$), chosen to increase L_M' at the expense of decreased reflectivity. The limiting value at high refractive-index discontinuity is $L_M'(\mathrm{LH}) \rightarrow n_1/[(1 - n_1/n_2)n_i]$ or $L_{\mathrm{LH,lim}} \approx \lambda_o$. So in the high-reflectivity region, the LH configuration has the larger L_M, usually around a wavelength. For case B the normalized mirror length L_M' can vary to zero for certain choices of n_2/n_1. These graphs do not show L_M' for smaller refractive-index ratios than these zeros; they will be discussed in more detail in Subsection 3.H.

For case A in Fig. 3(b), the curves increase rapidly as n_2/n_1 becomes smaller as a result of a pole in the expression for L_M. Equation (28) has a pole when $n_f/n_i = (n_2/n_1)^{2N}$, which turns out to be the same condition that forces $R \rightarrow 0$, providing an antireflection coating. For case A, the poles are at $n_2/n_1 = 1.05, 1.03, 1.02$ for $N = 4, 6, 11$, respectively. The reflectivity is plotted for $N = 6$ and this zero can be observed. Further exploration of these poles can be found in Subsection 3.H. For case B these values are $n_2/n_1 = 1.17, 1.10, 1.07$ for $N = 4, 6$, and 11, respectively. Now the zero in reflectivity ($N = 6$) is easily observable, but the poles in the curves for L_M are not shown because L_M occur before the zero is reached. The condition $L_M \rightarrow \infty$ cannot be measured because $R \rightarrow 0$ at those critical values of the refractive index. The traditional single-layer antireflection coating can be found from the condition for the pole by use of $N = 1$ and $n_2 = n_f$. Then $1/n_i = n_f/n_1^2$ so $n_1 = (n_i n_f)^{1/2}$. On either side of this pole, there could be large values of $|L_M|$ that might be observable even if R is small, as discussed next.

H. Condition for Zero Mirror Phase Dispersion ($L_M = 0$)

Figure 3(b) shows a condition that gives $L_M = 0$, which occurs when n_2 is chosen to be n_{20}, given by $n_f^2 = n_1 n_{20}(n_{20}/n_1)^{2N}$. This means that $\partial\varphi/\partial k = 0$ at this point; there is zero phase dispersion in the reflection. When $n_1 = 1.38$ and $n_f = 3.45$, the required ratio is $n_2/n_1 = 1.226$ for $N = 4$ and $n_2/n_1 = 1.151$ for $N = 6$. These zeros can be seen in Fig. 3 and are expanded to be clearer in Fig. 4. The reflectivity at zero phase dispersion is given by insertion of n_{20} into Eq. (31). In the limit of large N, it is straightforward to show that $R_0(N \text{ large}) = [(n_f n_i - n_1^2)/(n_f n_i + n_1^2)]^2$. This gives $R_0 = 0.09$ for the refractive indices given above. Thus zero phase dispersion typically does not occur with high reflectivity.

Figure 4 also shows the regions of $L_M < 0$. This is a regime of superluminal reflection, such as has been discussed within the context of photonic bandgap structures[9] and will be discussed further in another paper.

I. Solution for $N + 1/2$ Layer Pairs

When $N + 1/2$ layer pairs are used in a QWS, the resulting matrix is

$$M_{N+1/2} = (-1)^{N+1}\begin{bmatrix} \delta(a_N + b_N n_1) & -a_N/n_1 \\ n_1 d_N & \delta(d_N + c_N/n_1) \end{bmatrix}, \tag{35}$$

where a_N, b_N, c_N, and d_N are as given above. Using Eq. (27) and bearing in mind that $\delta \equiv \delta\vartheta$, we find that the length can be written as

$$L_{N+1/2} = \frac{\left[1 - \dfrac{n_1 n_2}{n_f^2}\left(\dfrac{n_1}{n_2}\right)^{2(N+1/2)}\right]\left[1 - \left(\dfrac{n_1}{n_2}\right)^{2(N+1/2)}\right]}{1 - \left(\dfrac{n_2 n_1}{n_f n_i}\right)^2\left(\dfrac{n_1}{n_2}\right)^{4(N+1/2)}} \times \frac{n_1 n_2}{n_i(n_2 - n_1)}\frac{\lambda_o}{4}. \tag{36}$$

The on-resonance reflectivity for $N + 1/2$ layer pairs can be calculated from Eq. (14) to obtain

$$R_{N+1/2} = \frac{[1 - (n_2 n_1/n_f n_i)(n_1/n_2)^{2(N+1/2)}]^2}{[1 + (n_2 n_1/n_f n_i)(n_1/n_2)^{2(N+1/2)}]^2}. \tag{37}$$

A comparison of results for N and $N + 1/2$ is shown in Fig. 5. As is well known, the extra half-layer

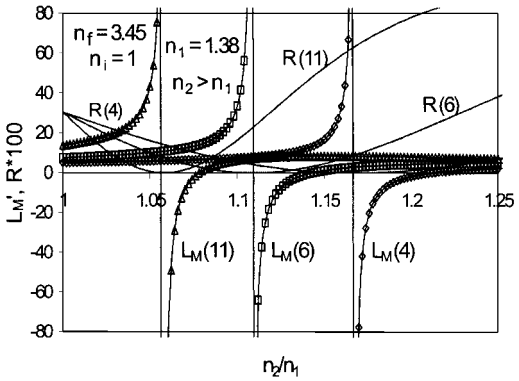

Fig. 4. Normalized optical mirror length for $n_1 = 1.38$ and a varying ratio of n_2/n_1 in the LH configuration, with a substrate refractive index of $n_f \equiv n_s = 3.45$ and an initial refractive index $n_i = 1$. Examples of $N = 4$, 6, and 11 layer pairs are shown. Also shown are the respective reflectivities R. This graph shows regions of zero and negative optical penetration length, as well as a region of large positive mirror length. The poles in the function are located at $R = 0$. The negative L_M corresponds to superluminal reflection, which can occur for small reflectivities.

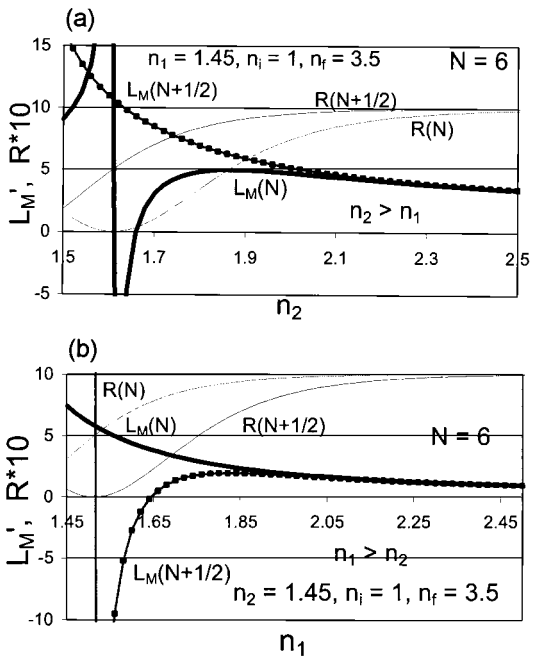

Fig. 5. Normalized optical mirror penetration length L_M' for $N = 6$ layer pairs, comparing N layer pairs (heavy line) and $N + 1/2$ layer pairs (ticked line). The scaled reflectivity is also shown as thin curves: (a) the LH configuration in which $N + 1/2$ layer pairs provide large reflectivity and remove the pole and (b) the HL configuration in which N layer pairs produce high reflectivity, and an additional layer reduces the reflectivity but introduces a pole.

introduces additional reflection that turns a low-reflectivity case [LH, as shown in Fig. 5(a)] into a high-reflectivity case. he values for L_M are changed as well; in the LH case, the extra half-layer removes the pole. The opposite is true for the HL case, as shown in Fig. 5(b); the extra half-layer introduces a pole.

4. Implications for the Fabry–Perot Free Spectral Range

It can be seen from Fig. 3 that, if the refractive indices are suitably chosen, the optical mirror length can be as large as $L_M' \approx 10$ or $L_M \approx 2.5\ \lambda_o$. This can lead to noticeable changes in cavity resonance spacing, as is known by those who design vertical-cavity structures that emit or detect light. Of course in this regime the reflectivity decreases because the dielectric layers have similar refractive indices. Nevertheless, the reflectivity calculated for the LH configuration with $n_f = 1.45$ and $N = 11$, at point $L_M' = 8$, which corresponds to $n_2/n_1 = 1.18$, gives a mirror reflectivity of $R_m = 86\%$.

In a FP filter the effective cavity length is increased by mirror lengths L_M:

$$L_{\text{eff}} = L_{\text{OPL}} + L_{M1} + L_{M2}. \tag{38}$$

As an example, consider a microelectrical-mechanical-tunable FP filter, such as reported in Ref. 4 with $L_{\text{OPL}} \approx 2\ \mu\text{m}$. If $L_M' = 4$ (or $L_M = \lambda_o$) for each mirror, then the effective cavity length for $\lambda_o = 1.55\ \mu\text{m}$ has more than doubled from 2 to 5.1 μm. This has important implications for the FSR. From Eqs. (5) and (6), the tuning range for this FP without including mirror phase dispersion is from 1.92 to 1.30 μm. If the mirror phase dispersion is included, the available tuning range varies from 1.68 to 1.44 μm, which is considerably smaller. If the LH ordering of refractive indices is used [Fig. 3(b)] with $N = 11$, $L_M' = 4$ is achievable when $n_2/n_1 = 1.5$ or $n_1 = 1.38$ and $n_2 = 2.07$. The reflectivity when $n_f = 3.45$ is $R = 0.998$, a practical regime to produce a high-finesse FP filter.

5. Conclusions

We found analytic forms for the on-resonance slope of the phase shift of a quarter-wave-stack mirror reflection. These slopes allowed us to present analytic expressions for the optical penetration length of light reflected from the mirror that are valid for any combination of refractive indices. The expressions differ depending on whether there are N or $N + 1/2$ layer pairs, but the results are similar, with the optical penetration length becoming larger as the reflectivity decreases. This makes good physical sense and is important for the calculation of mode spacing of a Fabry Perot filter and will be observed whenever the FP filter is thin, such as in a microelectrical-mechanical-tunable FP filter. We have also demonstrated a regime of negative optical path lengths, which is the regime of superluminal reflection in this reflecting photonic bandgap structure, will be further explained in another paper. The analytic approach in the frequency domain presented here can also be converted to the time domain to calculate the delay of light pulses that reflect from multilayer mirrors or photonic bandgap structures. A similar analysis can be carried out to analyze the time delay for the transmitted light.

This study was supported in part by Noyes Fiber Optical Systems and by the state of New Hampshire.

References

1. S. R. Mallinson and J. H. Jerman, "Miniature micromachined Fabry–Perot interferometers in silicon," Electron. Lett. **23,** 1041–1043 (1987).
2. E. C. Vail, G. S. Li, W. Yuen, and C. J. Chang-Hasnain, "GaAs micromachined widely tunable Fabry-Perot filters," Electron. Lett. **31,** 228–229 (1995).
3. A. T. T. D. Tran, Y. H. Lo, Z. H. Zhu, D. Haronian, and E. Mozdy, "Surface micromachined Fabry–Perot tunable filter," IEEE Photon. Technol. Lett. **8,** 393–395 (1996).
4. P. Tayebati, P. Wang, D. Vakhshoori, and R. N. Sacks, "Micro-electromechanical tunable filters with 0.47 nm linewidth and 70 nm tuning range," Electron. Lett. **34,** 76–78 (1998).
5. D. I. Babic and S. W. Corzine, "Analytic expressions for the reflection delay, penetration depth, and absorptance of quarter-wave dielectric mirrors," IEEE J. Quantum Electron. **28,** 514–524 (1992).
6. B. G. Kim and E. Garmire, "Comparison between the matrix method and the coupled-wave method in the analysis of Bragg reflector structures," J. Opt. Soc. Am. A **9,** 132–136 (1992).
7. B. G. Kim and E. Garmire, "Effect of front-facet reflections on the reflectivity of Bragg reflectors," Opt. Lett. **16,** 1065–1067 (1991).
8. L. R. Brovelli and U. Keller, "Simple analytical expressions for the reflectivity and penetration depth of a Bragg mirror between arbitrary media," Opt. Commun. **116,** 343–350 (1995).
9. S. Longhi, M. Marano, P. Laporta, M. Belmonte, and P. Crespi, "Experimental observation of superluminal pulse reflection in a double-Lorentzian photonic band gap," Phys. Rev. E **65,** 045602 (2002).
10. E. Garmire, "Optical nonlinearities in semiconductors," in *Nonlinear Optics in Semiconductors I*, E. Garmire and A. Kost, eds. (Academic, New York, 1999), p. 140.
11. M. Born and E. Wolf, *Principles of Optics*, 6th ed. (Pergamon, New York, 1980), pp. 52–70.
12. Z. Karim, C. Kyriakakis, A. R. Tanguay, Jr., K. Hu, L. Chen, and A. Madhukar, "Externally deposited phase-compensating dielectric mirrors for asymmetric Fabry–Perot cavity tuning," Appl. Phys. Lett. **64,** 2913–2915 (1994).